# Neighborhood and Haralick feature extraction for color texture analysis

***A. Porebski*[1, 2]*, N. Vandenbroucke*[1, 2] *and L. Macaire*[2]**
***alice.porebski@eipc.fr, nicolas.vandenbroucke@eipc.fr, ludovic.macaire@univ-lille1.fr***

(1) ***École d'Ingénieurs du Pas-de-Calais***
***Département Automatique***
***Campus de la Malassise***
***62967 Longuenesse Cedex - FRANCE***

(2) ***Laboratoire LAGIS - UMR CNRS 8146***
***Université des Sciences et Technologies de Lille***
***Cité Scientifique - Bâtiment P2***
***59655 Villeneuve d'Ascq - FRANCE***

## Abstract

*In this paper, we propose to study the influence of the neighborhood used to process the color co-occurrence matrices on the quality of texture analysis.*

*First, we measure the discriminating power of Haralick features extracted from the color co-occurrence matrices of color images coded in 28 different color spaces, and we select the most discriminating one for different 3x3 neighborhoods. Then, we experimentally verify that the most discriminating feature space, built by using an iterative selection procedure, depends on the chosen neighborhood and finally we study the impact of the neighborhood choice on the classification results by using the same feature space but different neighborhoods.*

*Experimental results achieved with the Barktek database have firstly shown the adequacy between the discriminating power of the selected feature space and the rate of well-classified images. We have also seen that the choice of the neighborhood does not highly influence the selection of the most discriminating feature but has a significant impact on the quality of discrimination between the considered textures. Indeed, we have worked with textures which contain vertical patterns and have shown that the best classification results have been obtained with horizontal neighborhoods. The choice of the neighborhood depends consequently on the analysed textures.*

## Introduction

The color texture classification consists in regrouping images whose textures are similar. Many authors have compared the color texture classification results obtained, on one hand thanks to grey scale analysis, and on the other hand, thanks to color texture features. They have shown that the analysis of color improves the rate of well-classified images and consequently the characterization of the different textures [1, 2, 3]. That is why many relevant features, initially defined in grey scale, have then been extended to color and used to classify color textures :

- Hernandez characterizes the different color texture classes of the Vistex benchmark database thanks to multispectral Markov random fields [4, 5].
- The extention to color of local binary patterns is used by Mäenpää and M. Pietikäinen for color textured image classification [2, 6].
- Arivazhagan, Sengur and Van de Wouwer analyse color textures thanks to features extracted from the wavelet transform [7, 8, 9].
- Palm builds a 96-dimensional feature space to characterize the color textures of the BarkTex benchmark database with the Haralick features extracted from color co-occurrence matrices [10, 11].

Like Drimbarean and Chindaro, Palm has compared the performances of texture classification reached by texture features extracted from images whose pixel color is represented in different color spaces [1, 3, 10]. Indeed the analysis of the color properties is not restricted to the acquisition color space $(R,G,B)$ and there exists a large number of color spaces which respect different properties [12]. These color spaces can be classified into four families : the primary color spaces, the luminance-chrominance color spaces, the perceptual color spaces and the independent color component spaces (see figure 1).

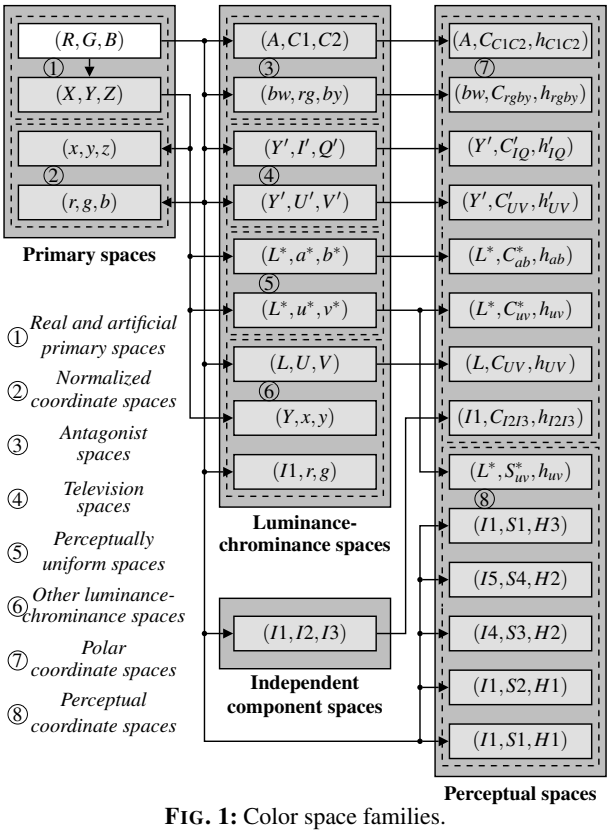


**FIG. 1:** Color space families.

In a previous study, we have seen that there does not exist any color space which is adapted to the classification of all kinds

of color textures [13]. That's why we have characterized the textures with features extracted from color images coded in each of the $N_S = 28$ different color spaces of figure 1. We have compared our classification results with those obtained by using only the $(R,G,B)$ space and have shown that the projection into different color spaces significantly improves the classification quality [13]. Moreover, it allows to work with a low-dimensional feature space.

In this paper, the color texture features used are Haralick features extracted from color co-occurrence matrices [14] (see second section). These matrices represent statistics on local interactions between the colors of pixels in a given neighborhood. We propose to study in this paper the influence of the neighborhood used to process the color co-occurrence matrices on the quality of texture analysis.
First, we measure the discriminating power, described in the third section, of each Haralick feature extracted from the color co-occurrence matrices of the color images coded in each of the $N_S$ considered color spaces, and we select the most discriminating one for different 3x3 neighborhoods.
We propose also to experimentally verify that the most discriminating feature space, built by using the iterative selection procedure described in the fourth section, depends on the chosen neighborhood and we study the impact of the neighborhood choice on the classification results.
Finally, we study the real influence of the neighborhood used to process the color co-occurrence matrices on the classification results by using the same feature space but different neighborhoods.
All these experiments are achieved with the color textures of the BarkTex benchmark database [11].

## Haralick features extracted from color co-occurrence matrices

Color co-occurrence matrices, introduced by Palm [10], are statistical features which both measure the color distribution in an image and consider the spatial interactions between the color of pixels. These matrices are defined for each color space denoted ($C_1$,$C_2$,$C_3$) of figure 1. Let $C_k$ and $C_{k'}$, be two of the three color components of this space ($k,k' \in \{1,2,3\}$) and $M^{C_k,C_{k'}}[\mathbf{I}]$, the color co-occurrence matrix which measures the spatial interactions between the color components $C_k$ and $C_{k'}$ of the pixels in the image $\mathbf{I}$. The cell $M^{C_k,C_{k'}}[\mathbf{I}](i,j)$ of this matrix contains the number of times that a pixel $P$ whose color component value $C_k(P)$ is equal to $i$, has, in its neighborhood denoted $\mathcal{N}$, a pixel $Q$ whose color component $C_{k'}(Q)$ is equal to $j$.

Figure 2 shows $N_N = 7$ different 3x3 neighborhoods $\mathcal{N}$ considered to compute the color co-occurrence matrices.

For a given neighborhood, the image $\mathbf{I}$ can be characterized by $N_M = 6$ color co-occurrence matrices : $M^{C_1,C_1}[\mathbf{I}]$, $M^{C_2,C_2}[\mathbf{I}]$, $M^{C_3,C_3}[\mathbf{I}]$, $M^{C_1,C_2}[\mathbf{I}]$, $M^{C_1,C_3}[\mathbf{I}]$ and $M^{C_2,C_3}[\mathbf{I}]$. Since the matrices $M^{C_2,C_1}[\mathbf{I}]$, $M^{C_3,C_1}[\mathbf{I}]$ and $M^{C_3,C_2}[\mathbf{I}]$ are respectively symmetric to the matrices $M^{C_1,C_2}[\mathbf{I}]$, $M^{C_1,C_3}[\mathbf{I}]$ and $M^{C_2,C_3}[\mathbf{I}]$, they are not used.

As they measure the local interaction between pixels, the color co-occurrence matrices are sensitive to significant differences of spatial resolution. To decrease this sensitivity, it is necessary to normalize these matrices by the total co-occurrence number $\sum_{i=0}^{N-1}\sum_{j=0}^{N-1} M^{C_k,C_{k'}}[\mathbf{I}](i,j)$, where $N$ is the quantification level number of the color components. The normalized color co-occurrence matrix $m^{C_k,C_{k'}}[\mathbf{I}](i,j)$ is defined by :

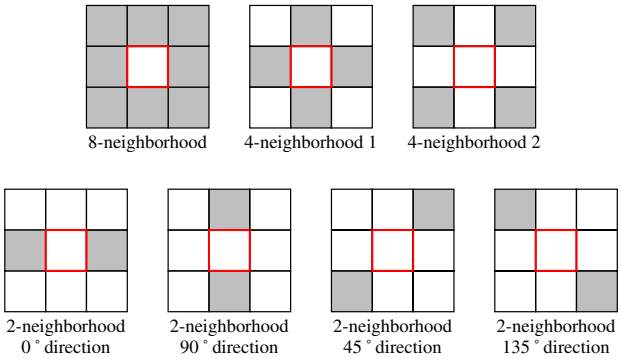


**FIG. 2:** 3x3 neighborhoods in which neighboring pixels are labeled as gray.

$$m^{C_k,C_{k'}}[\mathbf{I}](i,j) = \frac{M^{C_k,C_{k'}}[\mathbf{I}](i,j)}{\sum_{i=0}^{N-1}\sum_{j=0}^{N-1} M^{C_k,C_{k'}}[\mathbf{I}](i,j)}.$$

The color co-occurrence matrices characterize the color textures in the images. However, they cannot be easily exploited for color texture classification because they contain a large amount of information. To reduce it, while preserving the relevance of these descriptors, Haralick proposes to use $N_H = 14$ features, denoted $f_H^1$ to $f_H^{14}$, extracted from each matrix [14]. Consequently, an image is here characterized by $N_f = N_M \times N_H \times N_S = 6 \times 14 \times 28 = 2352$ color texture features $x^f$, $f = 1,\ldots,N_f$ (see figure 3).

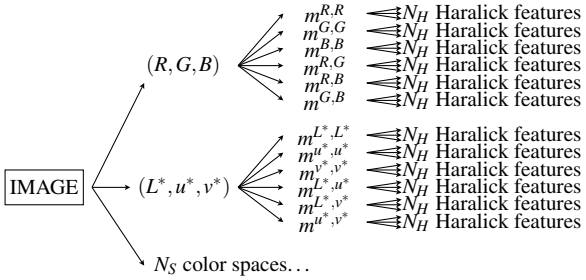


**FIG. 3:** Color texture features.

## Influence of the neighborhood on the selection of the most discriminating feature

First, we study the influence of the neighborhood $\mathcal{N}$ used to process the color co-occurrence matrices on the selection of the most discriminating texture feature. Indeed, since the total number $N_f$ of color texture features is very high, it is interesting to select the most discriminating one and to observe the impact of the neighborhood choice on the selection of this feature. This selection is done by measuring its discriminating power.

### *Feature discriminating power*

The discriminating power allows to sort the features according to their ability to discriminate the different texture classes. By considering each feature, the points characterizing the different classes form clusters projected on the corresponding axis. We choose the measures of cluster separability and compactness as being the discriminating power of each color texture feature.

The selection of the most discriminating feature is doing during a supervised learning scheme. At the first step of this learning, $N_\omega$ learning images $\omega_{i,j}$ $(i = 1,\ldots,N_\omega)$ which are representative of each of the $N_T$ texture classes $T_j$ $(j = 1,\ldots,N_T)$, are interactively selected by the user. The color texture features $x_{i,j}^f$ $(f = 1,\ldots,N_f)$ characterize each learning image $\omega_{i,j}$.
The measure of cluster compactness is defined by the within cluster scatter value $\Sigma_C^f$ :

$$\Sigma_C^f = \frac{1}{N_\omega \times N_T} \times \sum_{j=1}^{N_T} \sum_{i=1}^{N_\omega} (x_{i,j}^f - m_j^f)^2 \quad (1)$$

where $m_j^f$ is the mean value of the $f^{th}$ feature computed with the learning images $\omega_{i,j}$ of the class $T_j$.
The measure of the cluster separability is defined by the between cluster scatter value $\Sigma_S^f$ :

$$\Sigma_S^f = \frac{1}{N_T} \times \sum_{j=1}^{N_T} (m_j^f - m^f)^2 \quad (2)$$

where $m^f$ is the mean value of the $f^{th}$ feature for all the classes.
Then, the informational criterion $J^f$, which measures the discriminating power of each feature, is calculated and compared in order to select the most discriminating one for $N_T$ texture classes.
The informational criterion $J^f$ is expressed as :

$$J^f = \frac{\Sigma_S^f}{\Sigma_C^f + \Sigma_S^f} \quad (3)$$

When the clusters of points projected on the considered feature are well separated and compact, $J^f$ is close to 1. On the other hand, when the clusters corresponding to texture classes are mixed together, $J^f$ is close to 0.

## Experimental results

In order to examine the influence of the neighborhood $\mathcal{N}$ used to process the color co-occurrence matrices on the selection of the most discriminating texture features, experimental results are achieved with the color textures of the BarkTex database. After having described this benchmark database, the results of the selection of the three most discriminating color texture features for each neighborhood $\mathcal{N}$ will be presented and analysed. We will also examine the rate of well-classified images obtained with each most discriminating feature, for each neighborhood $\mathcal{N}$.

### BarkTex database

Color images of the BarkTex database are equally divided into 6 tree bark classes (see figure 4 : **Betula pendula** ($T_1$), **Fagus silvatica** ($T_2$), **Pica abies** ($T_3$), **Pinus silvestris** ($T_4$), **Quercus robus** ($T_5$), **Robinia pseudacacia** ($T_6$)). Each class regroups 68 images of size $128 \times 192$ yielding a collection of 408 images. To build the learning database, we have extracted $N_\omega = 32$ learning images $\omega_{i,j}$ of each texture class $T_j$.
For the classification, 36 request images for each texture class $T_j$ are used and these request texture images are classified thanks to the nearest neighbour classifier.

### Most discriminating texture feature

Table 1 shows, for each neighborhood $\mathcal{N}$, the three color texture features which maximize the discriminating power. For example, by considering the 8-neighborhood, the most discriminating feature is the eleventh Haralick feature $f_H^{11}$ extracted from the color co-occurrence matrix $M^{B,B}$ processed in the $(R,G,B)$ space. The discriminating power of this feature is equal to 0.673. The second most discriminating color texture feature, for this neighborhood, is the eleventh Haralick feature $f_H^{11}$ extracted from $M^{Y',h'_{UV}}$ processed in the $(Y',C'_{UV},h'_{UV})$ space whose

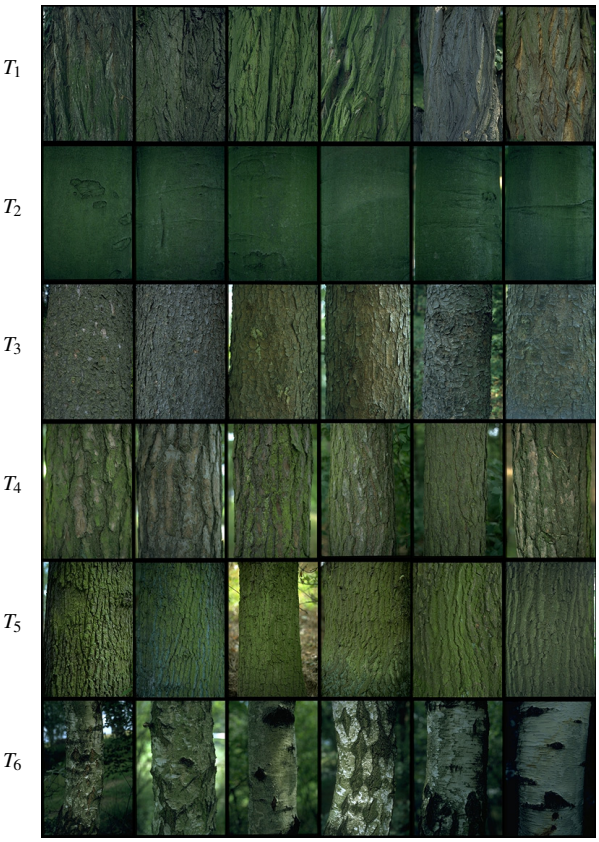


**FIG. 4:** Examples of BarkTex images

| Neighborhood $\mathcal{N}$ | Color space | Matrix | Haralick feature | Feature discriminating power | Classification result |
|---|---|---|---|---|---|
| 8-Neighborhood | $(R,G,B)$ | $M^{B,B}$ | $f_H^{11}$ | 0.672975 | 43.06% |
| | $(Y',C'_{UV},h'_{UV})$ | $M^{Y',h'_{UV}}$ | $f_H^{11}$ | 0.669566 | |
| | $(X,Y,Z)$ | $M^{Z,Z}$ | $f_H^{11}$ | 0.668019 | |
| 4-Neighborhood1 | $(R,G,B)$ | $M^{B,B}$ | $f_H^{11}$ | 0.678801 | 37.96% |
| | $(X,Y,Z)$ | $M^{Z,Z}$ | $f_H^{11}$ | 0.674867 | |
| | $(Y',C'_{UV},h'_{UV})$ | $M^{Y',h'_{UV}}$ | $f_H^{11}$ | 0.656066 | |
| 4-Neighborhood2 | $(Y',C'_{UV},h'_{UV})$ | $M^{Y',h'_{UV}}$ | $f_H^{11}$ | 0.678706 | 43.98% |
| | $(R,G,B)$ | $M^{B,B}$ | $f_H^{11}$ | 0.672635 | |
| | $(X,Y,Z)$ | $M^{Z,Z}$ | $f_H^{11}$ | 0.667671 | |
| 2-Neighborhood 0 ° direction | $(L^*_{uv},S^*_{uv},h^*_{uv})$ | $M^{L^*_{uv},S^*_{uv}}$ | $f_H^8$ | 0.653488 | 39.81% |
| | $(I1,r,g)$ | $M^{I1,g}$ | $f_H^8$ | 0.65258 | |
| | $(Y',C'_{UV},h'_{UV})$ | $M^{Y',h'_{UV}}$ | $f_H^{11}$ | 0.648573 | |
| 2-Neighborhood 90 ° direction | $(Y',C'_{UV},h'_{UV})$ | $M^{Y',h'_{UV}}$ | $f_H^{11}$ | 0.698544 | 34.26% |
| | $(Y',C'_{IQ},h'_{IQ})$ | $M^{h'_{IQ},h'_{IQ}}$ | $f_H^8$ | 0.661749 | |
| | $(Y',C'_{UV},h'_{UV})$ | $M^{h'_{UV},h'_{UV}}$ | $f_H^8$ | 0.66101 | |
| 2-Neighborhood 45 ° direction | $(Y',C'_{UV},h'_{UV})$ | $M^{Y',h'_{UV}}$ | $f_H^{11}$ | 0.696702 | 34.72% |
| | $(Y',C'_{UV},h'_{UV})$ | $M^{h'_{UV},h'_{UV}}$ | $f_H^8$ | 0.659814 | |
| | $(Y',C'_{IQ},h'_{IQ})$ | $M^{h'_{IQ},h'_{IQ}}$ | $f_H^8$ | 0.659438 | |
| 2-Neighborhood 135 ° direction | $(Y',C'_{UV},h'_{UV})$ | $M^{Y',h'_{UV}}$ | $f_H^{11}$ | 0.699047 | 35.19% |
| | $(Y',C'_{IQ},h'_{IQ})$ | $M^{h'_{IQ},h'_{IQ}}$ | $f_H^8$ | 0.662043 | |
| | $(Y',C'_{UV},h'_{UV})$ | $M^{h'_{UV},h'_{UV}}$ | $f_H^8$ | 0.66148 | |

**TAB. 1:** The three most discriminating color texture features and their associated discriminating power for each neighborhood $\mathcal{N}$.

discriminating power is equal to 0.6696.

This table shows also the rate of well-classified request images obtained with the most discriminating feature, for each neighborhood $\mathcal{N}$. For example, this rate reaches 43.06% by considering the eleventh Haralick feature $f_H^{11}$ extracted from the color co-occurrence matrix $M^{B,B}$ processed in the $(R,G,B)$ space.

### *Discussion*

By examining table 1, we can conclude that among the 14 Haralick features, only $f_H^8$ and $f_H^{11}$ which are respectively the sum and difference entropies, are selected whatever the considered neighborhood. These two features have not been considered by color texture classification procedures using Haralick features and proposed by Palm [10] and by Drimbarean et al [1]. These features should be taken into account by these procedures in order to improve their results.

Moreover, it is remarkable that whatever the chosen neighborhood, the eleventh Haralick feature $f_H^{11}$ extracted from $M^{Y',h'_{UV}}$ processed in the $(Y',C'_{UV},h'_{UV})$ space is always selected as one of the three most discriminating features among the 2352 candidate features.

Table 1 shows also that for the two 4-neighborhoods, the three features with the highest discriminating power are the same ones. So, the spatial arrangement of the neighbors in the 4-neighborhood does not influence the selection of the most discriminating features. The same conclusion arises for three of the four considered 2-neighborhoods. Only the features selected by considering the 0 ° direction are quite different from those determined by considering the three other directions. Indeed, since the examined textures contain vertical patterns, we expect that the 2-neighborhood based on 0 ° direction provides different results than those processed with the other directions.

Finally, by examining the classification results obtained with the most discriminating feature, for each neighborhood $\mathcal{N}$, we can notice that these classification results are very low. That is why it is interesting to extend the analysis to the multidimensional feature spaces.

## Influence of the neighborhood on the selection of the most discriminating feature space

The texture features previously selected are the most discriminating ones when they are considered individually, but the space formed by these features is not necessarily the most discriminating for the different texture classes because these features are often correlated.

We propose to determine the most discriminating feature space thanks to an iterative selection procedure processed during a supervised learning. This non-exhaustive procedure has given very good results by selecting an hybrid color space adapted to the considered images for color image segmentation [12].

### *Iterative selection*

At each step $d$ of the procedure, an informational criterion $J$ is calculated in order to measure the discriminating power of each candidate feature space. At the beginning of this procedure ($d = 1$), the $N_f$ one-dimensional candidate feature spaces, defined by each of the $N_f$ available color texture features, are considered. The candidate feature which maximizes $J$ is retained as being the best one for discriminating the texture classes (see table 1). This feature is selected at the first step and is associated at the second step of the procedure ($d = 2$) to each of the $(N_f - 1)$ remaining candidate color texture features in order to constitute $(N_f - 1)$ two-dimensional candidate feature spaces. We consider that the two-dimensional space which maximizes $J$ is the best space for discriminating the texture classes...

In order to only select color texture features which are not correlated, we measure, at each step $d \geq 2$ of the procedure, the correlation between each of the available color texture features and each of the $(d-1)$ other color texture features constituting the selected $(d-1)$ dimensional space. The considered features will be selected as candidate ones only if their correlation level with the color texture features already selected is lower than a threshold fixed by the user [12].

At each step $d$ of the procedure and for each of the $(N_f - d + 1)$ $d$-dimensional candidate feature spaces, we define, for the $i^{th}$ learning image $\omega_{i,j}$ $(i = 1,\ldots,N_\omega)$ associated to the texture class $T_j$ $(j = 1,\ldots,N_T)$, a color texture feature vector $X_{i,j} = [x_{i,j}^1,...,x_{i,j}^d]^{\mathrm{T}}$ where $x_{i,j}^d$ is the $d^{\mathrm{th}}$ color texture feature.
In order to measure the cluster compactness, defined by the within cluster scatter matrix $\Sigma_C$, equation 1 becomes :

$$\Sigma_C = \frac{1}{N_\omega \times N_T} \times \sum_{j=1}^{N_T} \sum_{i=1}^{N_\omega} (X_{i,j} - M_j)(X_{i,j} - M_j)^{\mathrm{T}} \tag{4}$$

where $M_j = [m_j^1,...,m_j^d]^{\mathrm{T}}$ is the mean vector of the $d$ color texture features of the class $T_j$.
In order to compute the cluster separability, defined by the between cluster scatter matrix $\Sigma_S$, equation 2 becomes :

$$\Sigma_S = \frac{1}{N_T} \times \sum_{j=1}^{N_T} (M_j - M)(M_j - M)^{\mathrm{T}} \tag{5}$$

where $M = [m^1,...,m^d]^{\mathrm{T}}$ is the mean vector of the $d$ color texture features for all the classes.
The most discriminating feature space maximizes the information criterion $J$ derived from equation 3 :

$$J = \mathrm{trace}\Big((\Sigma_C + \Sigma_S)^{-1}\Sigma_S\Big) \tag{6}$$

We retain a very simple stopping criterion which is the number of classes less one in order to compute the selected feature spaces with the same dimension.

### *Experimental results*

In order to examine the influence of the neighborhood $\mathcal{N}$ used to process the color co-occurrence matrices on the selection of the most discriminating feature space, experimental results are achieved with the BarkTex database. As it contains 6 texture classes, only the most discriminating 5-dimensional feature space is selected for each neighborhood $\mathcal{N}$.

#### *Most discriminating 5-dimensional feature space*

Table 2 shows the most discriminating 5-dimensional feature space for each neighborhood $\mathcal{N}$. For example, by considering the 8-neighborhood, the most discriminating 5-dimensional feature space contains :

- the eleventh Haralick feature $f_H^{11}$ extracted from the color co-occurrence matrix $M^{B,B}$ processed in the $(R,G,B)$ space,
- the tenth Haralick feature $f_H^{10}$ extracted from $M^{I1,I3}$ processed in the $(I1,I2,I3)$ space,
- the seventh Haralick feature $f_H^7$ extracted from $M^{I1,H3}$ processed in the $(I1,S1,H3)$ space,

| Neighborhood $\mathcal{N}$ | Color space | Matrix | Haralick feature | Feature space discriminating power and classification result |
|---|---|---|---|---|
| 8-Neighborhood | $(R,G,B)$ | $M^{B,B}$ | $f_H^{11}$ | |
| | $(I1,I2,I3)$ | $M^{I1,I3}$ | $f_H^{10}$ | 2.01415 |
| | $(I1,S1,H3)$ | $M^{I1,H3}$ | $f_H^{7}$ | |
| | $(L^*,u^*,v^*)$ | $M^{L^*,u^*}$ | $f_H^{9}$ | 72.22% |
| | $(I4,S3,H2)$ | $M^{I4,I4}$ | $f_H^{5}$ | |
| 4-Neighborhood1 | $(R,G,B)$ | $M^{B,B}$ | $f_H^{11}$ | |
| | $(I1,I2,I3)$ | $M^{I1,I3}$ | $f_H^{10}$ | 2.1052 |
| | $(L^*,u^*,v^*)$ | $M^{L^*,u^*}$ | $f_H^{9}$ | |
| | $(I5,S4,H2)$ | $M^{I5,H2}$ | $f_H^{5}$ | 75% |
| | $(I4,S3,H2)$ | $M^{I4,I4}$ | $f_H^{5}$ | |
| 4-Neighborhood2 | $(Y',C'_{UV},h'_{UV})$ | $M^{Y',h'_{UV}}$ | $f_H^{11}$ | |
| | $(Y',U',V')$ | $M^{Y',U'}$ | $f_H^{2}$ | 1.80271 |
| | $(x,y,z)$ | $M^{y,y}$ | $f_H^{11}$ | |
| | $(Y',C'_{IQ},h'_{IQ})$ | $M^{Y',h'_{IQ}}$ | $f_H^{2}$ | 64.35% |
| | $(L^*,C^*_{uv},h_{uv})$ | $M^{h_{uv},h_{uv}}$ | $f_H^{8}$ | |
| 2-Neighborhood 0 ° direction | $(L^*,S^*_{uv},h_{uv})$ | $M^{L^*,S^*_{uv}}$ | $f_H^{8}$ | |
| | $(I1,r,g)$ | $M^{I1,g}$ | $f_H^{12}$ | 2.23078 |
| | $(A,C1,C2)$ | $M^{C1,C1}$ | $f_H^{12}$ | |
| | $(L^*,C^*_{ab},h_{ab})$ | $M^{h_{ab},h_{ab}}$ | $f_H^{5}$ | 76.39% |
| | $(I1,C_{I2I3},h_{I2I3})$ | $M^{h_{I2I3},h_{I2I3}}$ | $f_H^{12}$ | |
| 2-Neighborhood 90 ° direction | $(Y',C'_{UV},h'_{UV})$ | $M^{Y',h'_{UV}}$ | $f_H^{11}$ | |
| | $(I1,S1,H3)$ | $M^{I1,H3}$ | $f_H^{7}$ | 1.78115 |
| | $(I1,I2,I3)$ | $M^{I1,I3}$ | $f_H^{10}$ | |
| | $(I5,S4,H2)$ | $M^{I5,S4}$ | $f_H^{5}$ | 54.17% |
| | $(L^*,C^*_{uv},h_{uv})$ | $M^{h_{uv},h_{uv}}$ | $f_H^{8}$ | |
| 2-Neighborhood 45 ° direction | $(Y',C'_{UV},h'_{UV})$ | $M^{Y',h'_{UV}}$ | $f_H^{11}$ | |
| | $(I1,S1,H3)$ | $M^{I1,H3}$ | $f_H^{7}$ | 1.78201 |
| | $(I1,I2,I3)$ | $M^{I1,I3}$ | $f_H^{10}$ | |
| | $(I5,S4,H2)$ | $M^{I5,S4}$ | $f_H^{5}$ | 55.09% |
| | $(L^*,S^*_{uv},h_{uv})$ | $M^{h_{uv},h_{uv}}$ | $f_H^{8}$ | |
| 2-Neighborhood 135 ° direction | $(Y',C'_{UV},h'_{UV})$ | $M^{Y',h'_{UV}}$ | $f_H^{11}$ | |
| | $(I1,S1,H3)$ | $M^{I1,H3}$ | $f_H^{7}$ | 1.78345 |
| | $(I1,I2,I3)$ | $M^{I1,I3}$ | $f_H^{10}$ | |
| | $(I5,S4,H2)$ | $M^{I5,S4}$ | $f_H^{5}$ | 56.02% |
| | $(L^*,S^*_{uv},h_{uv})$ | $M^{h_{uv},h_{uv}}$ | $f_H^{8}$ | |

**TAB. 2:** The most discriminating 5-dimensional feature spaces and the associated rate of well-classified images for each neighborhood $\mathcal{N}$.

- the nineth Haralick feature $f_H^9$ extracted from $M^{L^*,u^*}$ processed in the $(L^*,u^*,v^*)$ space,
- and the fifth Haralick feature $f_H^5$ extracted from $M^{I4,I4}$ processed in the $(I4,S3,H2)$ space.

The discriminating power of this 5-dimensional feature space is equal to 2.01415 and the rate of well-classified request images obtained with this feature space reaches 72.22%.

### *Discussion*

By examining table 2, we can firstly notice the adequacy between the discriminating power of the selected feature space and the rate of well-classified images since the higher the discriminating power is : the higher the well classification rate is.

Then, table 2 confirms that the 2-neighborhood based on 0 ° direction provides different results than those obtained with the other directions. Indeed, the 5-dimensional feature space selected by considering the 0 ° direction provides the highest discriminating power (2.23078) and the highest rate of well-classified request images (76.39%). The second best classification result is obtained by considering the 4-neighborhood1 which also contains the 0 ° direction neighborhood and the third one is obtained with the 8-neighborhood which also contains the horizontal direction.

The choice of the neighborhood is consequently very important since it allows to improve significantly the classification results.

## Influence of the neighborhood on the classification results

In order to study the real influence of the neighborhood used to process the color co-occurrence matrices on the classification results, we propose to examine the classification results obtained with the same feature space but with different neighborhoods.

### *Experimental results*

The influence of the neighborhood is studied by considering two different feature spaces. The first one, denoted "feature space 1", is the most discriminating feature space selected for the 8-neighborhood (see table 2) and the second one, denoted "feature space 2", is the most discriminating feature space selected for the 2-neighborhood based on 0 ° direction (see table 2).

#### *Classification results obtained with the feature spaces 1 and 2*

| Neighborhood $\mathcal{N}$ | Feature space 1 discriminating power and classification results | Feature space 2 discriminating power and classification results |
|---|---|---|
| 8-Neighborhood | 2.01415<br>72.22% | 1.31091<br>58.33% |
| 4-Neighborhood1 | 2.10776<br>74.07% | 1.73834<br>70.37% |
| 4-Neighborhood2 | 1.81922<br>62.04% | 1.06292<br>50.93% |
| 2-Neighborhood 0 ° direction | 2.04222<br>66.20% | 2.23078<br>76.39% |
| 2-Neighborhood 90 ° direction | 1.68695<br>56.94% | 0.890675<br>41.20% |
| 2-Neighborhood 45 ° direction | 1.68107<br>56.02% | 0.887254<br>43.52% |
| 2-Neighborhood 135 ° direction | 1.68933<br>56.02% | 0.878152<br>40.28% |

**TAB. 3:** The classification results obtained with the feature spaces 1 and 2 for each neighborhood $\mathcal{N}$.

Table 3 shows the rates of well-classified images obtained by considering the feature spaces 1 and 2. It indicates also the discriminating power associated to the considered feature space for each neighborhood $\mathcal{N}$. For example, the rate of well-classified images obtained by considering the feature space 1 reaches 74.07% for the 4-neighborhood1 and the discriminating power of this feature space is 2.10776 when the color co-

occurrence matrices are processed with this 4-neighborhood.

### *Discussion*

By examining the obtained results, we can notice the adequacy between the discriminating power of the feature space and the rate of well-classified images.

Table 3 also shows that the neighborhoods which contain horizontal neighbors provide the best discrimination between the considered texture classes : for the feature space 1, the best rates of well-classified request images are obtained with the 4-neighborhood1 (74.07%), then with the 8-neighborhood (72.22%) and thirdly by considering the $0^\circ$ direction (66.20%). For the feature space 2, the best classification results are obtained with the $0^\circ$ direction (76.39%), then with the 4-neighborhood1 (70.37%) and thirdly by considering the 8-neighborhood (58.33%).

## Conclusion

In this paper, we have presented experimental works in order to evaluate the influence of the neighborhood used to process the color co-occurrence matrices on the quality of texture analysis.

For this original purpose, we have firstly evaluated the relationships between the choice of the neighborhood and the selection of the most discriminating texture feature. We have also experimentally verified that the most discriminating feature space, built by using an iterative selection procedure, depends on the chosen neighborhood and finally we have studied the impact of the neighborhood choice on the classification results by using the same feature space whatever the considered neighborhood.

Experimental results achieved with the Barktek database have first shown the adequacy between the discriminating power of the selected feature space and the rate of well-classified images. We have also seen that the choice of the neighborhood does not highly influence the selection of the most discriminating feature but has a significant impact on the quality of discrimination between the textures. Indeed, we have worked with textures which contain vertical patterns and have shown that the best classification results have been obtained with the neighborhoods which contain the horizontal direction. The choice of the neighborhood depends consequently of the analysed textures.

## Acknowledgements

This research is funded by ”Pôle de Compétitivité Maud” and ”Région Nord-Pas de Calais”.

## Références

[1] A. Drimbarean and P.-F. Whelan, Experiments in colour texture analysis, Pattern Recognition, vol. 22, pp. 1161-1167, 2001.

[2] T. Mäenpää and M. Pietikäinen, Classification with color and texture : jointly or separately ?, Pattern Recognition, vol. 37, pp. 1629-1640, 2004.

[3] S. Chindaro, K. Sirlantzis and F. Deravi, Texture classification system using colour space fusion, Electronics Letters, vol. 41, pp. 589-590, 2005.

[4] O.J. Hernandez, J. Cook, M. Griffin, C. De Rama and M. McGovern, Classification of color textures with random field models and neural networks, Journal of Computer Science & Technology, vol. 5, pp. 150-157, 2005.

[5] R. Lakmann, VisTex benchmark database of color textured images, Universit Koblenz-Landau, http ://vismod.media.mit.edu/pub/VisTex/VisTex.tar.gz.

[6] M. Pietikäinen, T. Mäenpää and J. Viertola, Color texture classification with color histograms and local binary patterns, Texture02, pp. 109-112, 2002.

[7] S. Arivazhagan, L. Ganesan and V. Angayarkanni, Color texture classification using wavelet transform, ICCIMA'05 : Proceedings of the Sixth International Conference on Computational Intelligence and Multimedia Applications, pp. 315-320, 2005.

[8] A. Sengur, Wavelet transform and adaptive neuro-fuzzy inference system for color texture classification, Expert Systems with Applications, doi :10.1016/j.eswa.2007.02.032, 2007.

[9] G. Van de Wouwer, P. Scheunders, S. Livens and D. Van Dyck, Wavelet correlation signatures for color texture characterization, Pattern Recognition Letters, vol. 32, pp. 443-451, 1999.

[10] C. Palm, Color texture classification by integrative co-occurrence matrices, Pattern Recognition, vol. 37, pp. 965-976, 2004.

[11] R. Picard, C. Graczyk, S. Mann, J. Wachman, L. Picard and L. Campbell, BarkTex benchmark database of color textured images, Media Laboratory, Massachusetts Institute of Technology (MIT), Cambridge, ftp ://ftphost.uni-koblenz.de/outgoing/vision/Lakmann/BarkTex.

[12] N. Vandenbroucke, L. Macaire and J.-G. Postaire, Color image segmentation by pixel classification in an adapted hybrid color space. Application to soccer image analysis, Computer Vision and Image Understanding, vol. 90, pp. 190-216, 2003.

[13] A. Porebski, N. Vandenbroucke and L. Macaire, Iterative feature selection for color texture classification, In Proceeding of the 14th IEEE International Conference on Image Processing (ICIP'07), San Antonio, Texas, USA, vol. 3, pp. 509-512, 2007.

[14] R. Haralick, K. Shanmugan and I. Dinstein, Textural features for image classification, IEEE Transactions on Systems, Man and Cybernetics, vol. 3, pp. 610-621, 1973.

## Author Biography

*Alice Porebski, Engineer (Ecole d'Ingénieurs du Pas-de-Calais) is a PhD student at the Institute of Technology of the Université des Sciences et Technologies de Lille, France. Her research concerns color texture classification and quality control for an industrial application. This industrial application consists to analyse the color pattern glasses.*

*Nicolas Vandenbroucke received the PhD in computer science and control from the University of Lille in 2000. Since 2002, he is an associate professor in the Ecole d'Ingénieurs du Pas-de-Calais. He is a member of the LAGIS research laboratory (Laboratoire d'Automatique, Génie Informatique & Signal) in the "Vision and Image" group. His research interests include color representation, color image analysis applied to segmentation.*

*Ludovic Macaire received the M.S (Engineer) degree in Computer Science from the UTC Engineering school of Compiegne, France, in 1988 ; the PhD in computer science and control from the University of Lille in 1992, and the Habilitation à Diriger des Recherches from the University of Lille in 2004. Since 1993, he is an associate professor in the LAGIS Laboratory at the University of Lille. His research interests include color representation, color image analysis applied to segmentation and retrieval.*